

Supplemental Material

Table of Contents

Supplemental Figure 1. Baseline characteristics of MR^{B1-KO} mice.

Supplemental Figure 2. Characteristics of normal and MR^{B1-KO} mice after salt depletion and NCC blockade.

Supplemental Figure 3. Urinary analysis of MR^{B1-KO} mice after salt depletion and NCC blockade.

Supplemental Figure 4. Aldosterone-induced change in subcellular distribution of pendrin.

Supplemental Figure 5. Creation of mice with MR deletion in the entire nephron.

Supplemental Figure 6. Potassium depletion upon alkali loading induces concentrated distribution of pendrin label in the region of apical membrane.

Supplemental Figure 7. Pendrin regulation and salt-sensitive hypertension induced by aldosterone in NCC KO mice.

Supplemental Figure 8. The possible mechanism of thiazide-resistant hypertension.

Supplemental Figure 9. MR deletion in each cell types of aldosterone-sensitive distal nephron in MR^{B1-KO} mice.

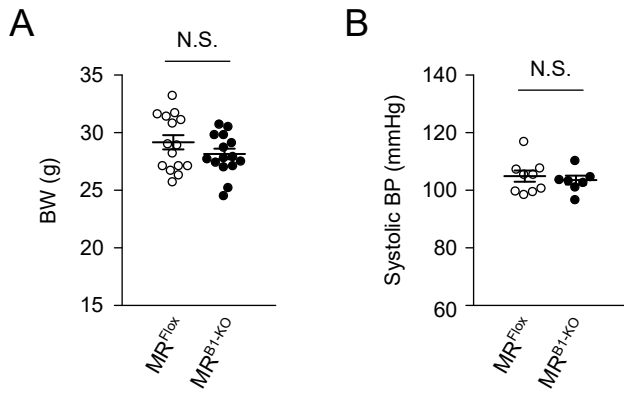
Supplemental Table 1. Primer pairs used for quantitative RT-PCR

Supplemental Table 2. Effects of amiloride and dietary potassium supplementation on systolic BP in C57BL/6J mice that were fed a high-salt diet and treated with aldosterone.

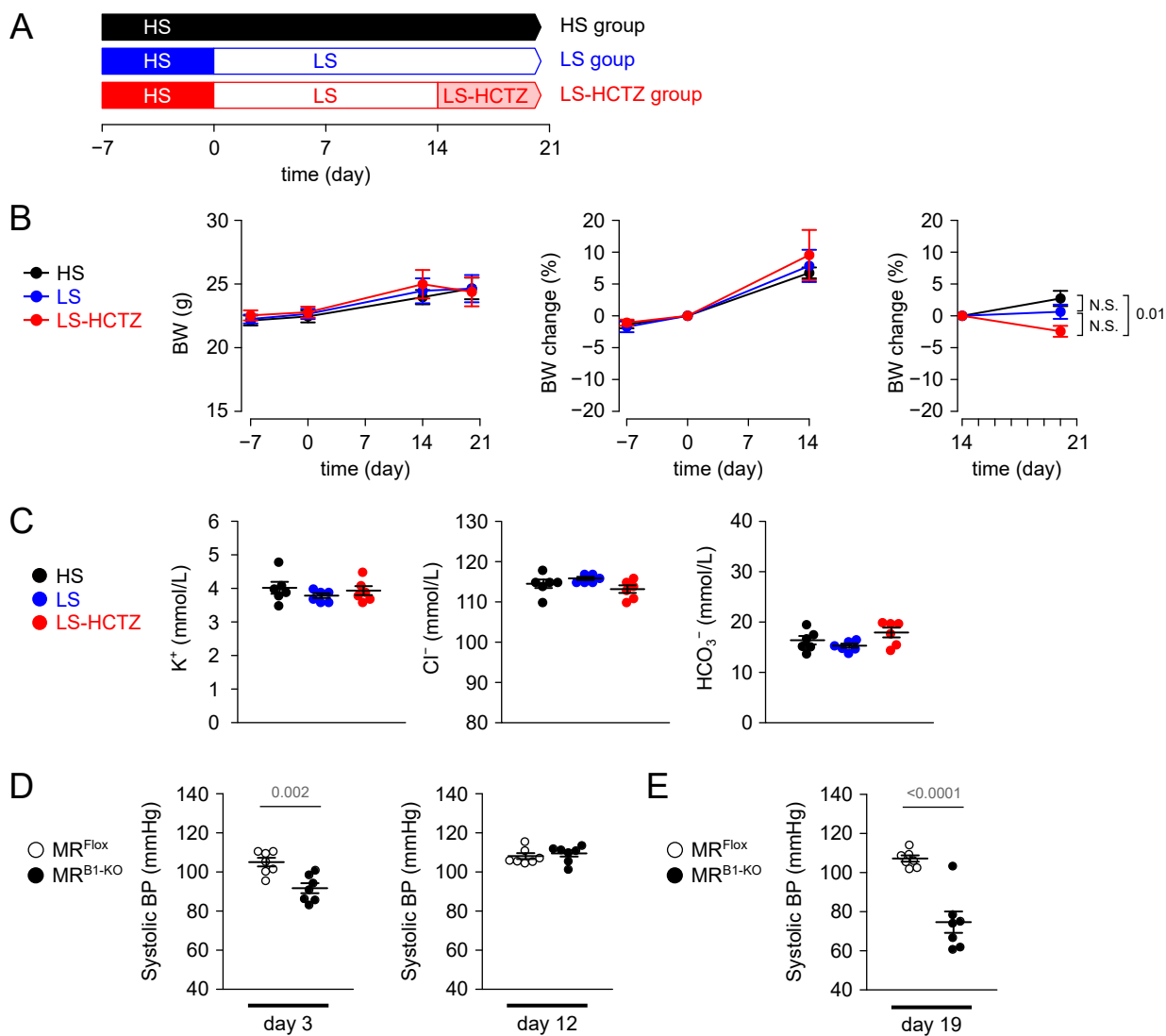
Supplemental Table 3. Systolic BP in MR^{Flox} mice and MR^{B1-KO} mice that were fed a high-salt diet and received either aldosterone treatment or no treatment.

Supplemental Table 4. Systolic BP in MR^{Control} and MR^{Pax8-KO} mice that were fed a high-salt diet and received either aldosterone treatment or no treatment.

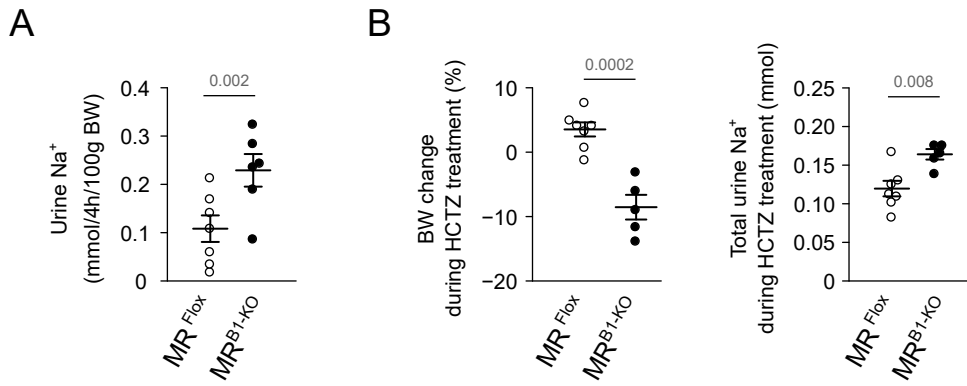
Supplemental Table 5. Systolic BP in MR^{B1-KO} mice fed a high-salt diet and treated with aldosterone either with or without dietary potassium supplementation.



Supplemental Figure 1. Baseline characteristics of MR^{B1-KO} mice. (A) Body weight (BW) of adult MR^{Fllox} mice and MR^{B1-KO} mice ($n = 15$ per group). N.S.: not significant. (B) Systolic blood pressure (BP) measured by the tail-cuff method in MR^{Fllox} mice and MR^{B1-KO} mice. ($n = 7-9$ per group). Data are expressed as mean \pm SEM. Statistical significance was analyzed with the unpaired t test.

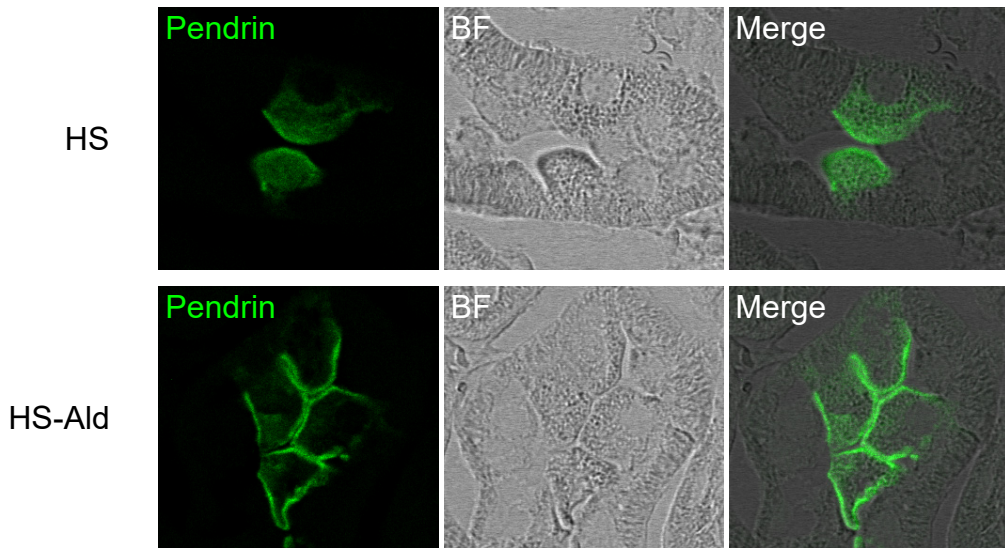


Supplemental Figure 2. Characteristics of normal and MR^{B1-KO} mice after salt depletion and NCC blockade. (A–C) Normal C57BL/6J mice were fed the high-salt diet (HS, 8% NaCl) for 1 week and then their nutrition was either switched to a low-salt diet (LS, 0.03% NaCl) or kept unchanged. After 2 weeks, the mice that were fed the LS diet either were treated with hydrochlorothiazide (HCTZ) for 6 days or received no treatment. (A) The schedule of the experiment. (B) The time course of BW changes (left), relative changes in BW before and after the salt depletion (middle), and relative changes in BW after add-on HCTZ treatment (right) (n = 6 per group). ANOVA, p = 0.01 (right). (C) Plasma concentrations of electrolytes on day 20 (n = 6 per group). (D and E) MR^{Flox} mice and MR^{B1-KO} mice were fed the HS diet for 1 week, then the LS diet for 2 weeks, and finally were treated with add-on HCTZ for 6 days. (D) Systolic BP was measured by the tail-cuff method on days 3 and 12 of the LS diet period (n = 7 per group). (E) Systolic BP was measured with the tail-cuff method on day 19 of the LS-HCTZ period (n = 7 per group). Data are expressed as mean ± SEM. Statistical significance was analyzed by ANOVA followed by the Tukey–Kramer *post hoc* test in (B and C) and the unpaired *t* test in (D and E); significant differences were indicated by horizontal bars with p values.

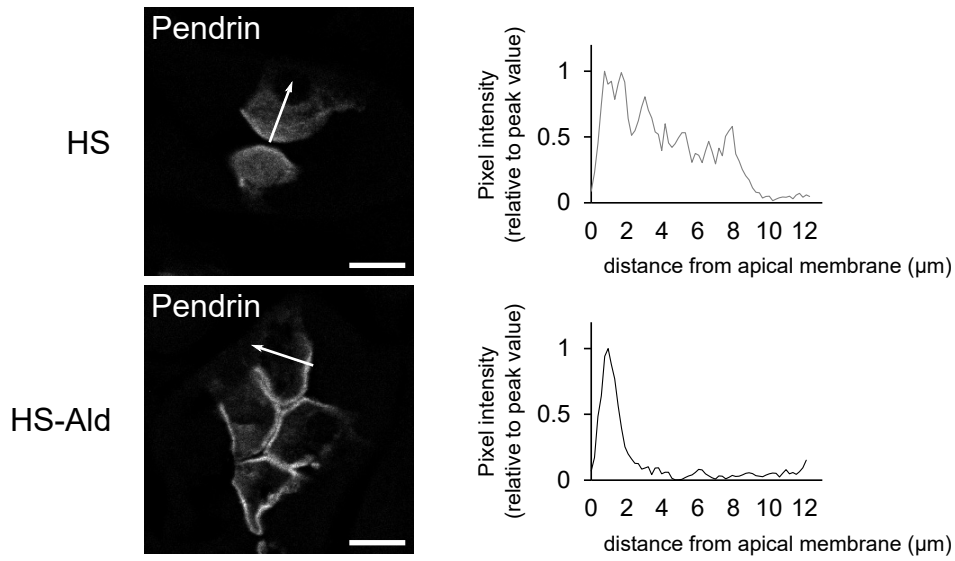


Supplemental Figure 3. Urinary analysis of MR^{B1-KO} mice after salt depletion and NCC blockade. (A) MR^{Flox} and MR^{B1-KO} mice were fed the LS diet for 2 weeks, and then they were injected with HCTZ. Urinary excretion of sodium in 4 hours after HCTZ injection are shown (n = 6–7 per group). (B) MR^{Flox} and MR^{B1-KO} mice were fed the LS diet for 2 weeks and then treated with add-on HCTZ for 6 days. BW change (left) and total amount of sodium excretion in urine (right) during the 6 days are shown (n = 5–7 per group). Data are expressed as mean ± SEM. Statistical significance was analyzed by the unpaired *t* test; significant differences were indicated by horizontal bars with *p* values.

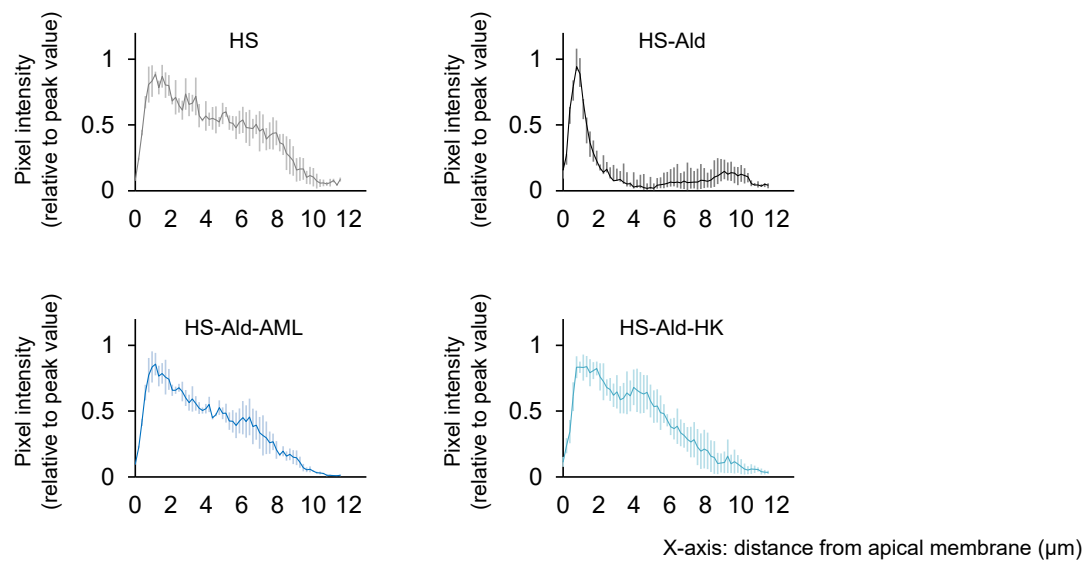
A



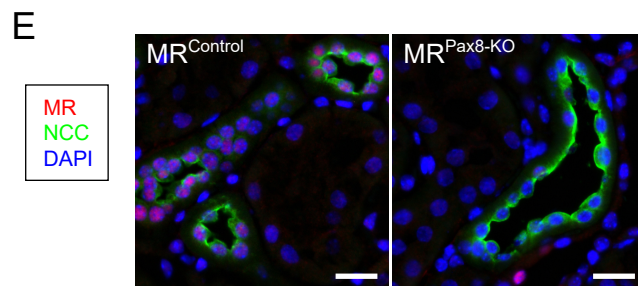
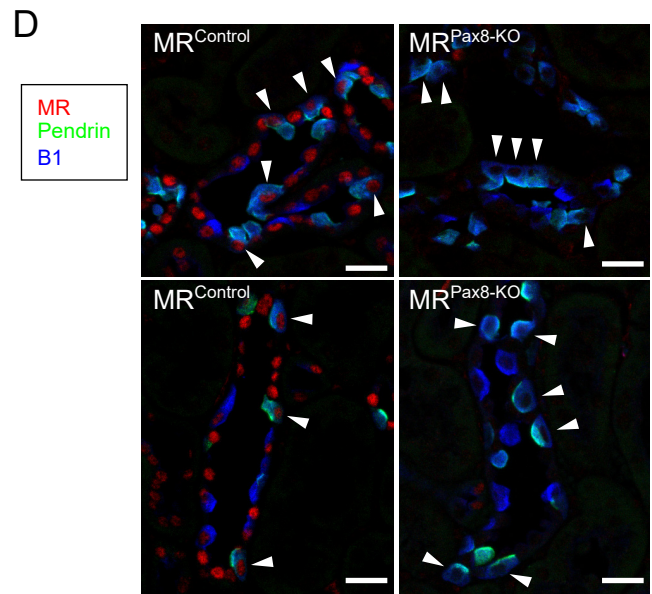
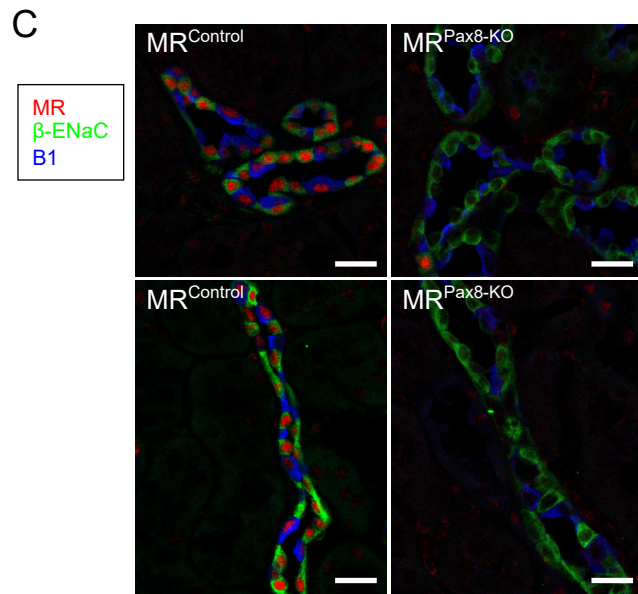
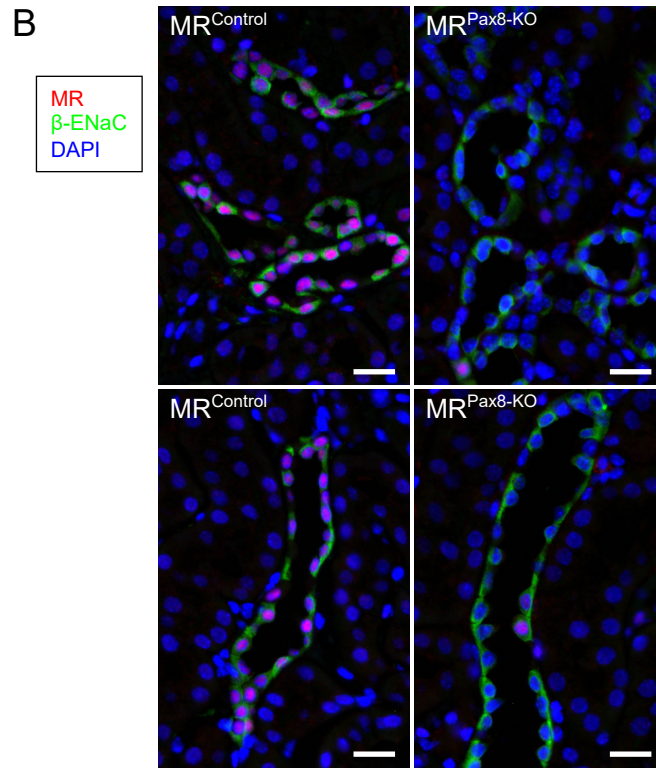
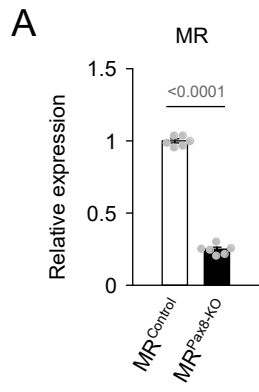
B



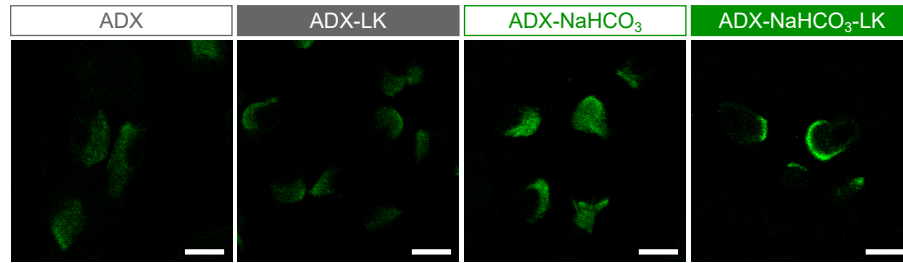
C



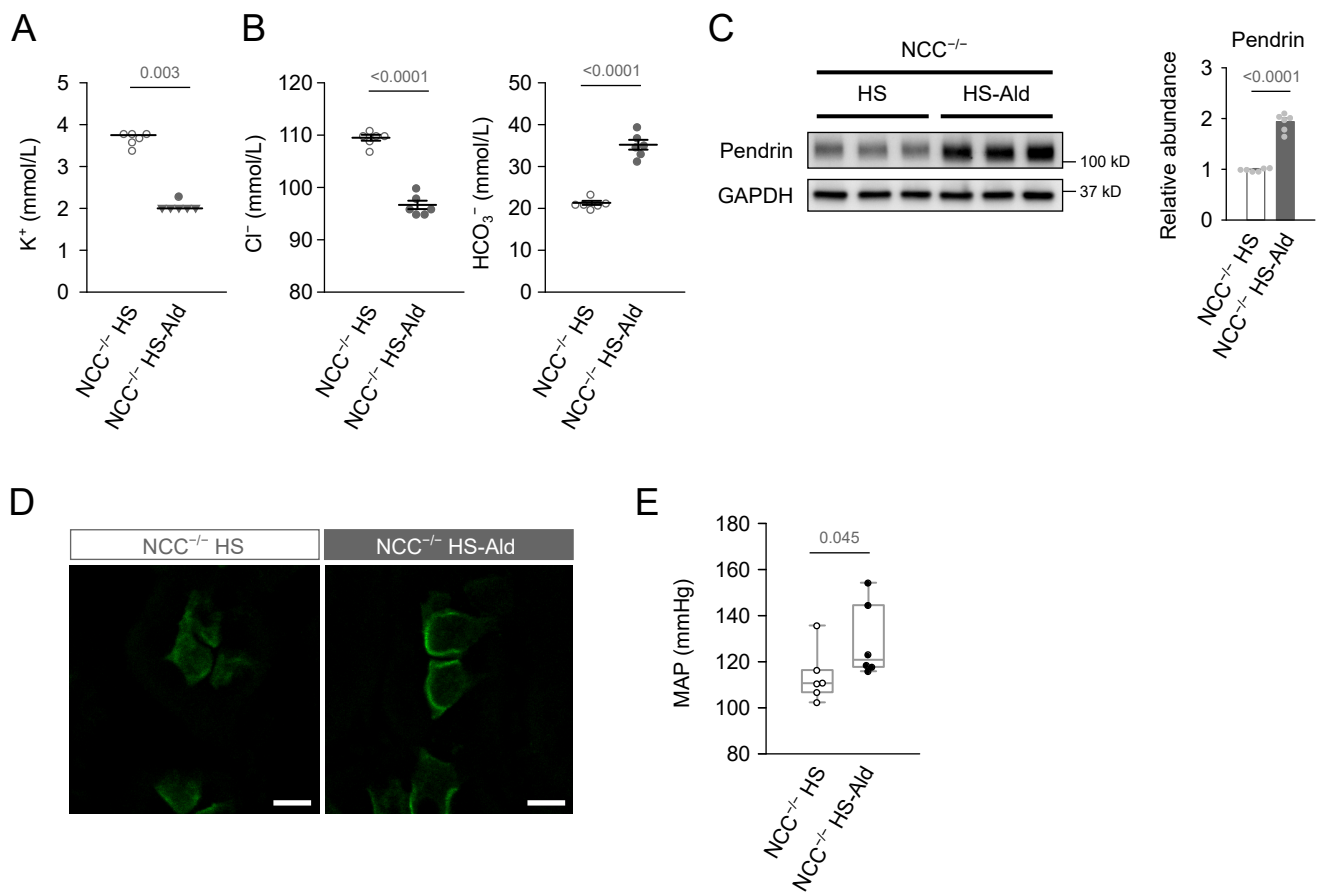
Supplemental Figure 4. Aldosterone-induced change in subcellular distribution of pendrin. C57BL/6J mice fed the high-salt diet (HS, 8% NaCl) either were treated with aldosterone (Ald, 200 μ g/kg per day, s.c.) or received no treatment for 14 days. Aldosterone treatment was combined with either amiloride (AML) or dietary potassium supplementation (high potassium, HK) or was administered alone. (A) Representative immunostaining of pendrin (green, left panels, corresponding to Figure 3C) and bright field (BF) image (gray, middle panels) are merged in right panels. Pendrin label is broadly distributed from the apical surface to the subapical cytosolic region in the HS group. The pendrin label is concentrated in the region of apical plasma membrane in HS-Ald group. (B) Representative curves of pixel intensity of pendrin label on a line from the apical surface to cytosolic region in HS and HS-Ald group (upper and lower, respectively). The intensity is normalized to the peak value in each curve. (C) Average curves of pixel intensity of pendrin label in 3 cells in each group. The aldosterone-induced change in subcellular distribution of pendrin label is reversed by AML and HK. Data are expressed as mean \pm SEM.



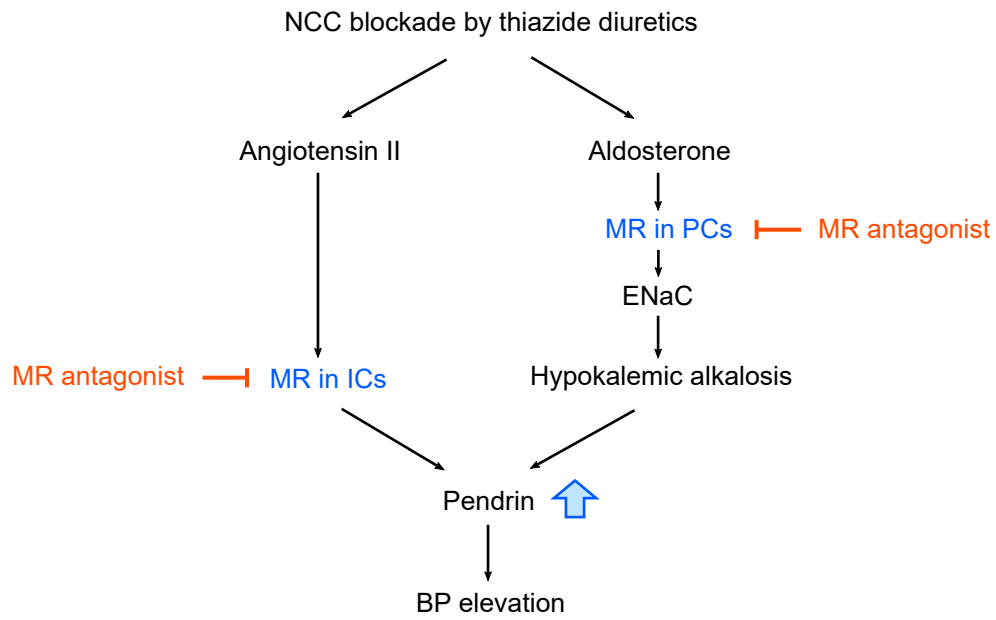
Supplemental Figure 5. Creation of mice with MR deletion in the entire nephron. MR deletion in the entire nephron was induced by doxycycline treatment of MR^{flox/flox};Pax8-rtTA^{+/-};tetO-cre^{+/-} mice (MR^{Pax8-KO} mice). (A) Quantitative analysis of MR gene expression in the kidneys. MR^{Pax8-KO} mice showed a large reduction in the renal expression of the MR gene as compared with uninduced control mice (MR^{Control}) (n = 6 per group). (B–E) Immunostaining revealed MR deletion in a large proportion of the cell population (80–90%) of MR-positive distal tubules, regardless of the cells types, in MR^{Pax8-KO} mice. Region of cortical labyrinth and near medullary ray are shown in upper and lower panel, respectively in (B–D). (B) Immunofluorescence staining of MR (red) with counterstaining of β -ENaC (green) for PCs, and DAPI (blue) for nuclei. (C) Immunofluorescence staining of MR (red) with counterstaining of β -ENaC (green) for PCs, and vacuolar H⁺-ATPase B1 subunit (B1, blue) for ICs. (D) Immunofluorescence staining of MR (red) with counterstaining of pendrin (green) for β -ICs and vacuolar H⁺-ATPase B1 subunit (B1, blue) for all ICs. Arrow heads indicate pendrin-positive and B1-positive β -ICs. (E) Immunofluorescence staining of MR (red) with counterstaining of NCC (green) for the detection of DCT cells. Data are expressed as mean \pm SEM. Statistical significance was analyzed by the unpaired *t* test in (A); significant differences were indicated by horizontal bars with p values. Scale bars, 10 μ m.



Supplemental Figure 6. Potassium depletion upon alkali loading induces concentrated distribution of pendrin label in the region of apical membrane. Adrenalectomized (ADX) C57BL/6J mice either were pretreated with NaHCO₃ loading (0.28 M in drinking water) for 3 days or received no pretreatment. They were then fed with either a low-potassium diet (LK) or normal diet for 4 days. Representative immunofluorescence staining of pendrin (green) of the kidneys. Scale bars, 10 μ m.

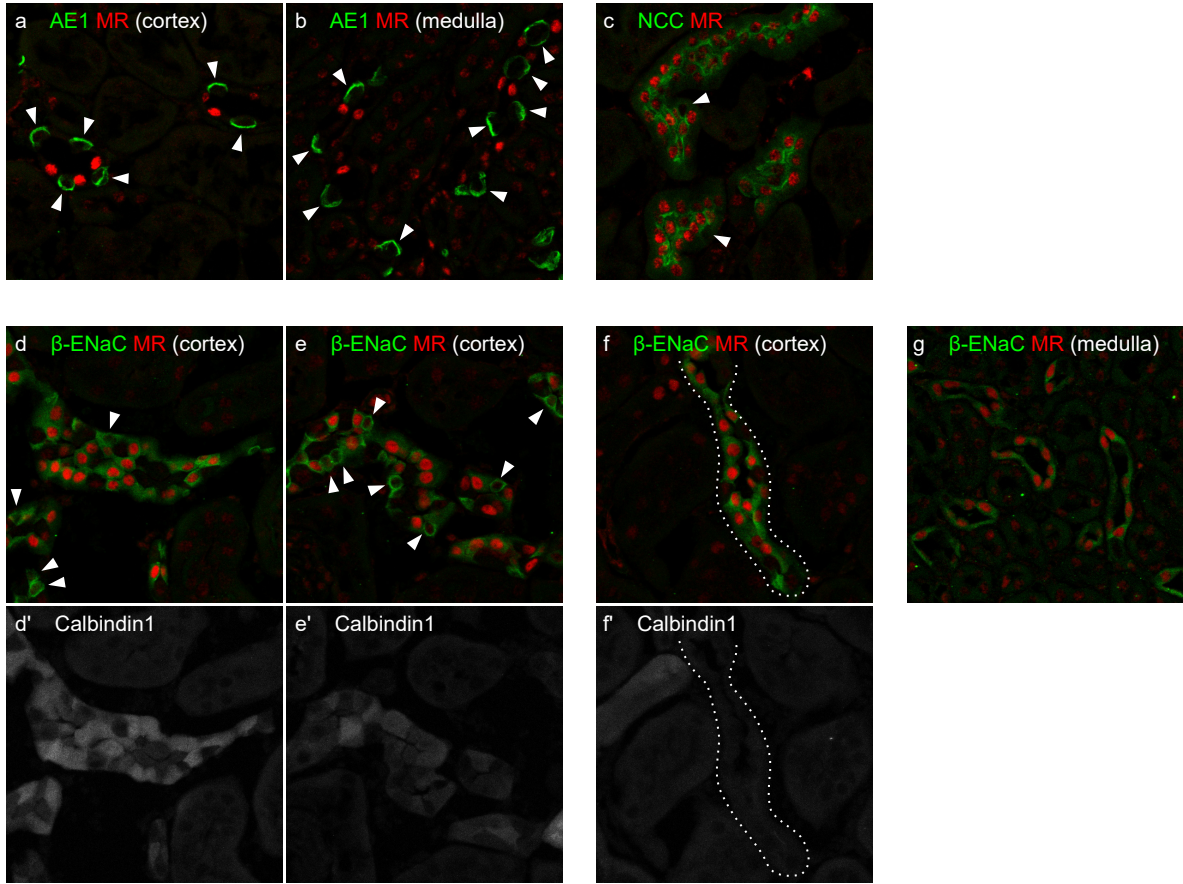


Supplemental Figure 7. Pendrin regulation and salt-sensitive hypertension induced by aldosterone in NCC KO mice. (A–E) NCC KO mice ($NCC^{-/-}$) fed a high-salt diet (HS, 2% NaCl) either were treated with aldosterone (Ald, 100 μ g/kg per day, s.c.) or received no treatment for 2 weeks. (A) Plasma concentration of potassium ($n = 6$ per group). Some values below the limit of detection (2 mmol/L) are presented as triangular plots. The horizontal bars indicate the median values in each group. (B) Plasma concentration of chloride and bicarbonate ($n = 6$ per group). (C) Representative immunoblots and quantities of pendrin in the kidney lysates ($n = 6$ per group). (D) Representative immunofluorescence staining of pendrin (green) of the kidneys. Scale bars, 10 μ m. (E) Box plots of telemetric measurement of MAP. Each dot represents the average values of hourly MAP over the last 2 days from each mouse ($n = 6$ per group). Data are expressed as mean \pm SEM in (B and C). Statistical significance was analyzed by Wilcoxon’s rank sum test in (A and E) and the unpaired t test in (B and C); significant differences were indicated by horizontal bars with p values.

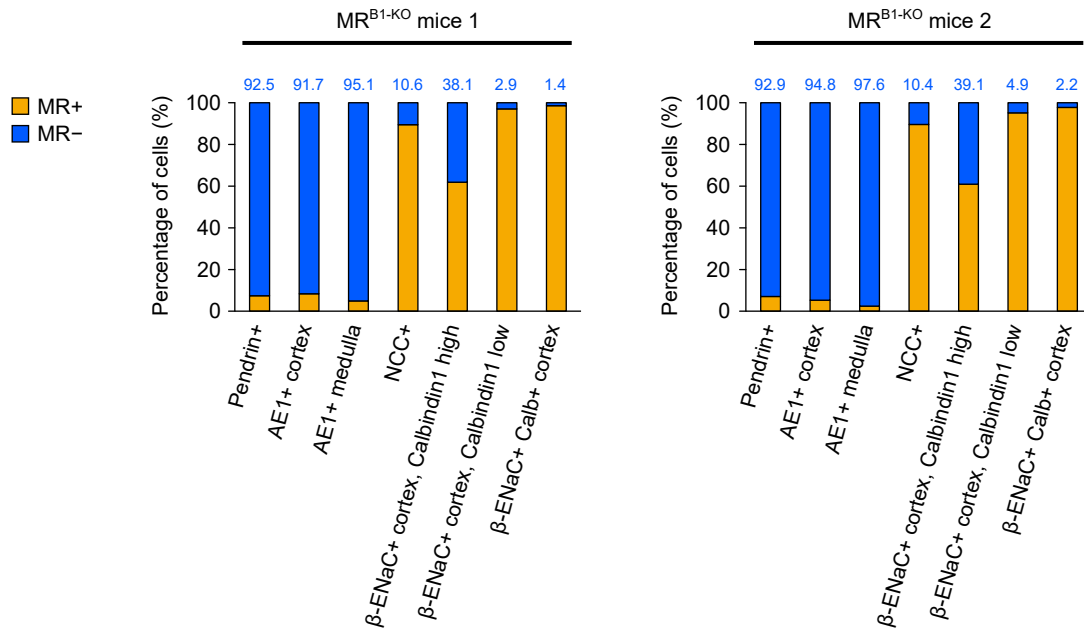


Supplemental Figure 8. The possible mechanism of thiazide-resistant hypertension.

A



B



Supplemental Figure 9. MR deletion in each cell types of aldosterone-sensitive distal nephron in MR^{B1-KO} mice. (A) Immunofluorescence staining of MR (red) with counterstaining of anion exchanger 1 (AE1) for α -ICs (green, panel a and b), NCC for DCT cells (green, panel c), and β -ENaC (green, panel d–g) for PCs in the kidney of MR^{B1-KO} mice. Panel d'–f' shows counterstaining of Calbindin1 (gray) in d–f. Arrow heads shows cells in which MR is deleted. MR is deleted in α -ICs that show basolateral expression of AE1, in cortex (a) and medulla (b). MR deletion is observed in small population of NCC-positive DCT cells (c). In cortex, β -ENaC-positive tubules that have rather high expression of Calbindin1 are observed mainly in cortical labyrinth (d, d', e, and e'), and supposed as connecting tubules. Other β -ENaC-positive tubules in cortex that have low expression of Calbindin1 are mainly found near the medullary rays, and assumed as cortical collecting ducts (f and f'). MR is deleted in some part of β -ENaC-positive cells in Calbindin1-high tubules (d and e). On the other hand, MR is not deleted in β -ENaC-positive cells in Calbindin1-low tubules (f, surrounded by dotted line). MR deletion is not observed in β -ENaC-positive cells in medullary collecting ducts (g). (B) The percentage of MR deleted cells in each cell types of aldosterone-sensitive distal nephron was calculated by counting cells in a transverse section of kidney in two individual MR^{B1-KO} mice. The blue values indicate the percentage of MR-deleted cells in each cell type.

Supplemental Table 1. Primer pairs used for quantitative RT-PCR

Gene	Primer Pair (5'-3')	
<i>Nr3c2</i> (encoding MR)	Forward	ATGGGTACCCGGTCCTAGAG
	Reverse	ACCAAGCAGATCTTGGAAGG
<i>Rps29</i>	Forward	GGAGTCACCCACGGAAGTT
	Reverse	ATGAAGCCTATGTCCTTCGC

Supplemental Table 2. Effects of amiloride and dietary potassium supplementation on systolic BP in C57BL/6J mice that were fed a high-salt diet and treated with aldosterone.

	HS	HS-Ald	HS-Ald-AML	HS-Ald-HK
Systolic BP (mmHg)	97 ± 3	121 ± 2 *	100 ± 3 †	102 ± 3 ††
n	6	6	6	6

Data are expressed as mean ± SEM. Statistical significance was analyzed by ANOVA followed by the Tukey–Kramer *post hoc* test. ANOVA, $p < 0.0001$. * $p < 0.0001$ vs the HS group; † $p = 0.0001$ vs the HS-Ald group; †† $p = 0.0004$ vs the HS-Ald group. Systolic BP was measured with the tail-cuff method.

Supplemental Table 3. Systolic BP in MR^{Flox} mice and MR^{B1-KO} mice that were fed a high-salt diet and received either aldosterone treatment or no treatment.

	MR^{Flox}	MR^{Flox}	MR^{B1-KO}	MR^{B1-KO}
	HS	HS-Ald	HS	HS-Ald
Systolic BP (mmHg)	101 ± 2	115 ± 2 *	103 ± 3	116 ± 4 †
n	8	10	5	9

Data are expressed as mean ± SEM. Statistical significance was analyzed by ANOVA followed by the Tukey–Kramer *post hoc* test; ANOVA, $p = 0.001$. * $p = 0.009$ vs the MR^{Flox}-HS group; † $p = 0.04$ vs the MR^{B1-KO}-HS group. Systolic BP was measured by the tail-cuff method.

Supplemental Table 4. Systolic BP in MR^{Control} and MR^{Pax8-KO} mice that were fed a high-salt diet and received either aldosterone treatment or no treatment.

	MR ^{Control}	MR ^{Pax8-KO}	MR ^{Control}	MR ^{Pax8-KO}
	HS	HS	HS-Ald	HS-Ald
Systolic BP (mmHg)	102 ± 2	101 ± 2	118 ± 3 *	107 ± 3 †
n	5	5	6	6

Data are expressed as mean ± SEM. Statistical significance was analyzed using ANOVA followed by the Tukey–Kramer *post hoc* test; ANOVA, $p = 0.0002$. * $p = 0.0006$ vs the MR^{Control}-HS group; † $p = 0.008$ vs the MR^{Control}-HS-Ald group. Systolic BP was measured with the tail-cuff method.

Supplemental Table 5. Systolic BP in MR^{B1-KO} mice fed a high-salt diet and treated with aldosterone either with or without dietary potassium supplementation.

	MR ^{B1-KO} -HS-Ald	MR ^{B1-KO} -HS-Ald-HK
Systolic BP (mmHg)	111 ± 2	98 ± 1 *
n	7	7

Data are expressed as mean ± SEM. Statistical significance was evaluated by the unpaired *t* test; * $p < 0.0001$ vs MR^{B1-KO}-HS-Ald group. Systolic BP was measured by the tail-cuff method.